JOURNAL OF VIROLOGY, Dec. 2009, p. 12204–12214 Vol. 83, No. 23
0022-538X/09/$12.00 doi:10.1128/JVI.01103-09

Regulation of Proinflammatory Cytokine Expression in Primary Mouse Astrocytes by Coronavirus Infection▽

Dongdong Yu, Hongqing Zhu, Yin Liu, Jianzhong Cao, and Xuming Zhang*

Departments of Microbiology and Immunology, University of Arkansas for Medical Sciences, Little Rock, Arkansas 72205-7199

Received 29 May 2009/Accepted 14 September 2009

Previous studies have shown that proinflammatory cytokines, such as tumor necrosis factor alpha (TNF-α) and interleukin 6 (IL-6), are differentially induced in primary mouse astrocytes by mouse hepatitis virus strain A59 (MHV-A59) and MHV-2. However, the signaling events that trigger TNF-α and IL-6 induction in these cells upon MHV infection remain unknown. In this study, we explored the potential signaling events. We found that induction of TNF-α and IL-6 occurred as early as 2 h postinfection and was completely dependent on viral replication. Using inhibitors specific for three mitogen-activated protein kinases, we showed that induction of TNF-α and IL-6 by MHV-A59 infection was mediated through activation of the Janus N-terminal kinase signaling pathway, but not through the extracellular signal-regulated kinase or p38 signaling pathway. This finding was further confirmed with knockdown experiments using small interfering RNAs specific for Janus N-terminal kinase. Interestingly, while nuclear factor κB (NF-κB), a key transcription factor required for the expression of proinflammatory cytokines in most cell types, was activated in astrocytes during MHV-A59 infection, disruption of the NF-κB pathway by peptide inhibitors did not significantly inhibit TNF-α and IL-6 expression. Furthermore, experiments using chimeric viruses demonstrated that the viral spike and nucleocapsid proteins, which play important roles in MHV pathogenicity in mice, are not responsible for the differential induction of the cytokines. These results illustrate the complexity of the regulatory mechanism by which MHV induces proinflammatory cytokines in primary astrocytes.

Proinflammatory cytokines are a group of cytokines that were originally identified as mediators of inflammation. However, further studies have found that many proinflammatory cytokines have multiple biological functions, e.g., regulating cell development, maintaining homeostasis, and antiviral effects. Tumor necrosis factor alpha (TNF-α) is one such proinflammatory cytokine that has diverse biological effects, including cytolysis, cytotoxicity, immunoregulation, cellular proliferation, and antiviral responses, and thus plays important roles in the pathogenesis of inflammatory diseases (15, 34, 36, 38, 39). TNF-α has also been considered to be a contributing factor in the human disease multiple sclerosis, a degenerative disease of the central nervous system (CNS) (14), although the precise role of TNF-α in multiple sclerosis remains controversial (31, 35).

In the CNS, TNF-α is produced by resident astrocytes and microglia or by infiltrating blood-borne macrophages and other mononuclear cells during disease and mediates cell injury in nerve cells and oligodendrocytes (24, 40). Depending on the types of cells and stimuli, TNF-α can be expressed through diverse pathways, and its expression is regulated at multiple levels. For example, lipopolysaccharide induces TNF-α in microglia through p38 mitogen-activated protein (MAP) kinase at both the transcriptional and translational levels (21), while interleukin 1β (IL-1β) induces TNF-α and IL-6 in astrocytes through a mechanism involving protein kinase C at the transcriptional level (4), although p38 can also modulate TNF-α expression at the translational level (21). Production of TNF-α by astrocytes stimulated with Newcastle disease virus is achieved by transcriptional activation and mRNA stabilization through protein kinase C (11). Furthermore, it has been shown that different MAP kinases are involved in different cell types in TNF-α production (6, 20).

Mouse hepatitis virus (MHV) can infect rodents and cause digestive and CNS diseases that range from acute fulminant fatal encephalitis to chronic demyelination. However, the severity of CNS disease is significantly influenced by both viral genetics and host factors. For example, MHV strain JHM (or MHV type 4 [MHV-4]) is highly neurovirulent, causing acute lethal encephalitis, although a number of variants, naturally occurring or laboratory-adapted mutants, exhibit various degrees of neurovirulence (7, 16). Strain MHV-A59 has relatively low neurovirulence, causing less encephalitis and more demyelination (18, 19). In contrast, strain MHV-2 has low neurovirulence, causing only mild meningitis but no encephalitis and demyelination (8, 12, 47). Host factors, including innate and adaptive immunities, have been shown to be critical in the development of MHV-caused CNS diseases (25, 37, 41). MHV infection induces the expression of a number of proinflammatory cytokines and chemokines in the mouse CNS (1, 17, 23, 30, 42). Although the exact roles of individual cytokines in MHV pathogenesis are not completely understood, in general, the level and kinetics of their expression are correlated with the severity of the CNS disease (23, 30). TNF-α mRNA is induced more rapidly in mouse CNSs infected with a lethal MHV strain than in those infected with a nonlethal MHV variant (30). In vivo experiments have shown that the cytokines TNF-α, IL-6, and IL-1β are expressed by astrocytes in mice chronically infected with MHV-JHM and that these activated astrocytes are localized to areas of virus infection and demyelination (43).

* Corresponding author. Mailing address: Department of Microbiology and Immunology, University of Arkansas for Medical Sciences, 4301 W. Markham Street, Slot 511, Little Rock, AR 72205. Phone: (501) 686-7415. Fax: (501) 686-5359. E-mail: zhangxuming@uams.edu.

▽ Published ahead of print on 23 September 2009.

However, the severity and pathology of CNS disease caused by the MHV-JHM strain are similar in recipient mice with passively transferred $CD8^+$ T cells derived from wild-type and TNF-α knockout mice (31), suggesting that $CD8^+$ T-cell-mediated TNF-α does not play a significant role in CNS pathogenesis. Interestingly, infection of primary astrocytes and microglia with MHV-A59 induces both mRNA and protein expression (23, 49), while infection of primary peritoneal macrophages with MHV-JHM induced only mRNA transcription but inhibited translation (42). Thus, expression of TNF-α by MHV infection is virus strain and cell type dependent and can be regulated at both the transcriptional and translational levels.

Previously, we and others showed that infection of primary mouse astrocytes and microglia with MHV-A59 significantly induced the expression of proinflammatory cytokines, especially TNF-α and IL-6, while infection with MHV-2 did not (23, 49). However, the signaling events that trigger TNF-α and IL-6 induction in these cells upon MHV infection remain unknown. In the current study, we explored the molecular mechanisms by which MHV infection induces TNF-α and IL-6 expression in primary mouse astrocytes. We found that the induction of TNF-α and IL-6 by MHV-A59 is mediated by activation of the Janus N-terminal kinase (JNK) signaling pathway, but not by the extracellular signal-regulated kinase and p38 MAP pathways. Interestingly, while nuclear factor κB (NF-κB), which is a key transcription factor required for the expression of proinflammatory cytokines in most cell types, was activated in astrocytes during MHV-A59 infection, NF-κB activation appears to be dispensable for MHV-induced TNF-α expression. Furthermore, experiments using chimeric viruses demonstrated that the spike (S) and nucleocapsid (N) proteins, which play important roles in MHV pathogenicity in mice, are not responsible for the differential induction of the cytokines.

MATERIALS AND METHODS

Viruses, cells, and reagents. MHV-A59 and MHV-2 were used throughout this study. Both viruses were originally obtained from Michael Lai (University of Southern California Keck School of Medicine, Los Angeles, CA). The recombinant virus Penn-98-1 was kindly provided by Ehud Lavi (University of Pennsylvania School of Medicine). Penn-98-1 was made by targeted recombination between MHV-A59 and a synthetic subgenomic RNA containing the S gene of MHV-2. Thus, Penn-98-1 has the MHV-2 S gene in the genome background of MHV-A59 (9). The recombinant virus icA59/2N was generated using a reverse-genetics method as described below. It contains the MHV-A59 genome with the N gene replaced with its counterpart from MHV-2. All viruses were plaque purified for three rounds, propagated in the mouse astrocytoma cell line DBT (13), and purified by ultracentrifugation before being used for infection throughout this study. Virus titers were determined by plaque assay in DBT cells. The p38 kinase inhibitor SB203580 and its nonspecific control inhibitor SB202474, the MEK nonspecific control inhibitor UO124, and the JNK inhibitor SP600125 were purchased from Calbiochem Inc., while the MEK inhibitor UO126 was purchased from Promega. The stock solutions for these inhibitors were prepared in dimethyl sulfoxide and stored at −20°C. The NF-κB inhibitors SC3060 and NF-κB p65 (Ser276)-inhibitory peptide were purchased from Santa Cruz Biotechnology Inc. and Imgenex Co., respectively. The stock solutions of 5 mM for these peptides were prepared in distilled water and stored at −20°C.

Virus purification and inactivation. Viruses were grown in DBT cells overnight. The culture medium and cell lysates were collected following freezing and thawing once and clarified of cell debris by centrifugation at 3,000 × *g* for 30 min at 4°C (Marathon 3200R; Fisher Scientific). For virus purification, the clarified virus preparation was loaded onto a 30% (wt/vol) sucrose cushion and centrifuged at 27,000 rpm for 3 h at 4°C in an SW27/28 rotor (Beckman). The pellets that contained the virus were resuspended in phosphate-buffered saline (PBS). To inactivate the virus, the virus preparations were exposed to UV light for 30 min on ice in a UV cross-linker (Fisher Scientific). The effectiveness of inactivation was confirmed by the absence of cytopathic effect and virus infectivity after inoculation of DBT cell monolayers with UV-irradiated virus.

Preparation of mouse primary glial cells. Mouse primary glial cells were isolated from the brains of neonatal C57BL/6 mice by using a technique exploiting the differential adherence characteristics of astrocytes, microglia, and oligodendrocytes. Mice were euthanized with halothane, and their brains were removed aseptically and immediately placed in ice-cold PBS. The meninges were removed, and the brains were homogenized through a vacuum filtration apparatus fitted with a 100-μm nylon mesh. The cells were resuspended in defined Dulbecco minimum essential medium containing 500 mg/liter glucose supplemented with 10% fetal bovine serum, 200 mM L-glutamine, 100 U/ml penicillin, 0.1 mg/ml streptomycin and cultured in 75-cm^2 flasks for 9 to 14 days until the monolayers reached confluence. The confluent cultures were vigorously agitated on a rotary shaker for 15 h (37°C; 200 rpm) to dislodge the microglia and oligodendrocytes. The resulting cell suspension, rich in microglia, was transferred to 75-cm^2 culture flasks and allowed to adhere at 37°C. After a 3-h adherence interval, loosely adherent cells and cells in suspension (most of which were oligodendrocytes) were removed by gently shaking the flasks at room temperature. The astrocytes remained attached to the culture flask after the initial microglial-dissociation step. The purity of the isolated glial cells was determined by immunohistochemical staining with cell-type-specific antibodies. This isolation procedure routinely yielded cell populations with a purity of >95%. All experiments involving the use of mice were conducted in accordance with the guidelines of the Institutional Animal Care and Use Committee at the University of Arkansas for Medical Sciences.

Immunofluorescence assay. For determination of the purity of the isolated astrocytes, cells were cultured on coverslips, fixed with 4% paraformaldehyde, and permeabilized with 0.3% Triton X-100. Following incubation with 10% normal goat serum, the cells were stained with a primary rabbit anti-glial fibrillary acidic protein (GFAP) (Dako Cytomation) antibody (1:100 dilution) and a secondary goat anti-rabbit immunoglobulin G antibody conjugated with fluorescein isothiocyanate (Sigma Co., St. Louis, MO; 1:100 dilution). The stained cells were washed with PBS, and the coverslips were mounted on slides with an aqueous mounting medium. The cells were then observed under a fluorescence microscope (model IX70; Olympus). For detection of NF-κB, the same immunofluorescence assay was carried out, except that the primary antibody was a rabbit anti-NF-κB p65 polyclonal antibody (Santa Cruz; 1:100 dilution).

ELISA. The Quantikine enzyme-linked immunosorbent assay (ELISA) system (R&D Systems) was used for the detection and quantification of TNF-α and IL-6 according to the manufacturer's instructions. Briefly, primary astrocytes were infected with MHVs at a multiplicity of infection (MOI) of 5. The culture supernatants were collected at various time points postinfection (p.i.) and used for determining the protein levels of TNF-α and IL-6. ELISA was performed in 96-well plates that were precoated with a polyclonal antibody specific for mouse TNF-α or IL-6. The plate was incubated with the culture supernatants and controls for 2 h at room temperature and then washed with a wash buffer five times. The mouse TNF-α conjugate was added to each well and incubated for an additional 2 h, followed by five washes. The substrate solution was added to each well and incubated for 30 min. The reaction was stopped by the addition of a stop solution. The plate was read by a microplate reader (Spectra Max 190; Molecular Devices) at 450 nm, and 540 nm was used as a correction. The cytokine protein concentration was obtained based on a standard curve generated by performing parallel assays using known amounts of TNF-α or IL-6 (included in the kits).

RNA isolation and qRT-PCR. Total RNAs were isolated from primary astrocytes using TriZol reagent and treated with DNase I (Invitrogen, Carlsbad, CA) prior to being used in quantitative real-time reverse transcription-PCR (qRT-PCR). Primers for TNF-α, IL-6, and β-actin and 6-carboxytetramethylrhodamine TaqMan probes were synthesized by Applied Biosystems Inc. (Foster City, CA). The forward and reverse primers were 5′-ACA AGG CTG CCC CGA CTA C-3′ and 5′-TGG AAG ACT CCT CCC AGG TAT ATG-3′ for TNF-α and 5′-CCC AAT TTC CAA TGC TCT CC-3′ and 5′-TCC ACA AAC TGA TAT GCT TAG G-3′ for IL-6, respectively. The primer pair for β-actin was 5′-GGC TAT GCT CTC CCT CAC G-3′ (forward) and 5′-CGC TCG GTC AGG ATC TTC AT-3′ (reverse). The RT reaction was carried out using the iScript cDNA synthesis kit (Bio-Rad Laboratories) according to the manufacturer's instructions. Real-time PCRs were performed in a total reaction volume of 25 μl using the iCycler kit (Bio-Rad Laboratories) containing a final concentration of 400 nM of forward and reverse primers, 200 nM of TaqMan probe, and 1 μl of cDNA from the RT step. The results were analyzed using the iCycler IQ multicolor real-time PCR detection system (Bio-Rad Laboratories). The gene expression levels in various

experimental groups were calculated after the cycle thresholds against the β-actin housekeeping gene were normalized and are presented as picogram values.

Western blot analysis. Western blot analysis was carried out to examine JNK pathway activation. Primary murine astrocytes were infected with MHV strains at an MOI of 5. At 24 h p.i., the cells were washed five times with PBS and lysed with a radioimmunoprecipitation assay buffer (20 mM Tris, pH 7.5, 150 mM NaCl, 1% NP-40, 0.5% sodium deoxycholate, 1 mM EDTA, 0.1% sodium deoxyl sulfate) containing proteinase inhibitors. Intracellular proteins in the lysates were separated by electrophoresis on 10% polyacrylamide gels and were then transferred to nitrocellulose or polyvinylidene difluoride membranes. After being blocked with 5% nonfat milk in TBST buffer (10 mM Tris-Cl [pH 7.5], 150 mM NaCl, 0.1% Tween 20) for 1 h at room temperature, the membranes were incubated overnight at 4°C with a monoclonal antibody specific for the JNK, phosphor-JNK, c-Jun, or phosphor-c-Jun (1:1,000 dilution; Cell Signaling Technology, Inc.) in TBST-milk. Primary antibodies to total p38, phosphor-p38, total MEK, and phosphor-MEK were purchased from Cell Signaling Technology, Inc. Following extensive washing of the membranes with TBST buffer for 10 min, horseradish peroxidase-conjugated anti-mouse or anti-rabbit secondary antibodies (1:2,000 dilution; Cell Signaling Technology, Inc.) were added, and the reaction mixture was incubated for 1 h at room temperature. Proteins were detected using the Renaissance Western blot chemiluminescence reagent (NEN), followed by exposure to X-ray film (Kodak).

Assay for NF-κB activation. NF-κB activation was analyzed with the TransAM NF-κB p65 transcription factor assay kit according to the manufacturer's protocol (Active Motif, Inc.). Briefly, cell nuclear extracts were incubated with the immobilized oligonucleotide containing the NF-κB p65 consensus site (5′-GGG ACT TTC C-3′) in a 96-well plate for 1 h, and the plate was washed three times. A primary antibody specific for NF-κB p65 was then added, followed by incubation for 1 h, and the plate was subsequently washed three times. Following the addition of a secondary anti-immunoglobulin G antibody conjugated with horseradish peroxidase and incubation for 1 h, the reaction mixture was incubated with a developing solution for 30 min and the reaction was stopped by the addition of a stop solution. The protein-DNA binding complex was then quantified by spectrophotometry. Wild-type and mutated consensus oligonucleotides were used for competitive binding with NF-κB to monitor the specificity of the assay. The wild-type oligonucleotide competed for NF-κB binding to the probe immobilized on the plate, and the mutated consensus oligonucleotide did not. These controls were included in each assay.

Generation of recombinant MHV-A59/2N virus. The parental MHV-A59 (icA59) and the recombinant MHV-A59/MHV2N (icA59/2N) viruses were generated from infectious cDNA clones by using the reverse-genetics method established by Yount et al. (48). Recombinant icA59/2N has the MHV-A59 genome with replacement of the N gene from MHV-2. The seven cDNA fragments (A to G) encompassing the entire genome of the wild-type MHV-A59 were kindly provided by Ralph Baric (University of North Carolina at Chapel Hill). For generation of icA59/2N, the G fragment, which contained all of the structural genes in the 3′ one-third of the viral genome, was divided into two roughly equal fragments (G1 and G2) and separately subcloned into plasmid vector pCR2.1-TOPO (Invitrogen), which can be joined together using the restriction enzyme Esp3I site. The MHV-2 N gene was amplified from viral RNAs by RT-PCR using the primer pair 5′-GGC GTC TCA AAG ACA GAA AAT CTA AA-3′ (forward primer) and 5′-TTA TCG ACT TAG GTT CTC AAC AAT G-3′ (reverse primer). The N gene of MHV-A59 in the G2 fragment was then replaced with the MHV-2 N gene using the unique enzyme restriction sites SalI and NotI, resulting in a chimeric G2-MHV-2N fragment. Following restriction enzyme digestion and gel purification, the chimeric fragment and the other cDNA clones of MHV-A59 origin were ligated together in a total reaction volume of 200 μl overnight at 16°C. Following extraction with chloroform and precipitation with isopropanol, the ligated DNAs were used for in vitro transcription with the mMessage mMachine T7 transcription kit (Ambion). The reaction was performed in 50-μl reaction mixtures supplemented with 7.5 μl of 30 mM GTP at 40.5°C for 25 min, 37.5°C for 50 min, and 40.5°C for 25 min. The transcription products were electroporated into BHK cells expressing the MHV receptor and cocultured with DBT cells as described previously (48). The resultant infectious virus, termed icA59/2N, was recovered from the culture medium and propagated in DBT cells following three rounds of plaque purification.

Statistical analysis. The data were analyzed for statistical significance by analysis of variance when necessary and were expressed as mean values ± standard deviations. The mean values were compared using Student's *t* test. *P* values of <0.01 or <0.05 were considered statistically significant.

RESULTS

Differential induction of TNF-α and IL-6 in primary astrocytes by infections with MHV-A59 and MHV-2. Using the cytometrics bead array assay, which can detect six proinflammatory cytokines (monocyte chemoattractant protein 1, IL-12p70, IL-6, IL-10, gamma interferon, and TNF-α) simultaneously, we previously showed that only TNF-α and IL-6 were differentially induced by MHV-A59 and MHV-2 (49). To verify these findings and to further understand the signaling mechanisms, here we used ELISA to quantify the cytokines in primary mouse astrocytes. The purity of the isolated astrocytes was determined to be >95% by immunofluorescence analysis with an antibody specific for GFAP (Fig. 1A). The primary astrocytes were then infected with MHV-A59 or MHV-2 at an MOI of 5. Culture supernatants collected at 24 h p.i. were used for ELISA. Although certain variations were noted between data obtained from the cytometrics bead array assay and ELISA (data not shown), there was general agreement between the two methods with respect to TNF-α and IL-6. Approximately 1,400 pg/ml of TNF-α and 470 pg/ml of IL-6 were secreted into the culture medium in MHV-A59-infected astrocytes, while less than 200 pg/ml of TNF-α and 10 pg/ml of IL-6 were induced by MHV-2 infection. In mock-infected cells, both TNF-α and IL-6 were either undetectable (Fig. 1B and C) or detected at a very low level (Fig. 1E and F), indicating that normal cell culture conditions have little effect on cytokine induction.

To determine whether the differential induction was due to different replication abilities of the two virus strains, culture supernatants were analyzed for the virus titer by plaque assay. The results showed that the two viruses had similar yields (Fig. 1D). Thus, the differential induction of TNF-α and IL-6 in primary astrocytes was not due to the replication efficiencies of the two viruses. To further determine which stages of the virus life cycle are involved in cytokine induction, astrocytes were infected with both live and UV-inactivated MHVs. At 24 h p.i., the culture supernatants were analyzed for TNF-α and IL-6 proteins by ELISA. The results showed that UV-inactivated MHV could no longer induce TNF-α and IL-6 (Fig. 1E and F, respectively), demonstrating that virus replication is required for triggering TNF-α and IL-6 induction. The results also confirmed that the purified virus preparation was devoid of any potential inducers for the cytokines from DBT cell cultures.

Kinetics of TNF-α and IL-6 induction by MHV-A59 infection. To understand whether the induction of the cytokines is regulated at the transcriptional level, we employed qRT-PCR to determine the cytokine mRNAs and found that both TNF-α and IL-6 mRNAs were significantly induced in MHV-A59-infected, but not in MHV-2-infected, astrocytes at 24 h p.i. (data not shown). To further determine the kinetics of TNF-α and IL-6 induction, intracellular RNAs were isolated from astrocytes at various times p.i., and the levels of TNF-α and IL-6 mRNAs were quantified by qRT-PCR. As shown in Fig. 2A and B, both TNF-α and IL-6 mRNAs were detected as early as 2 h p.i. at levels of approximately 1 and 2 pg, respectively. They then increased rapidly and reached a plateau by 4 h p.i., at which time approximately 8 pg of TNF-α and IL-6 mRNAs per 10^5 cells was detected. Thereafter, they decreased rapidly. By 12 h p.i., only half of the mRNAs detected at 4 h p.i.

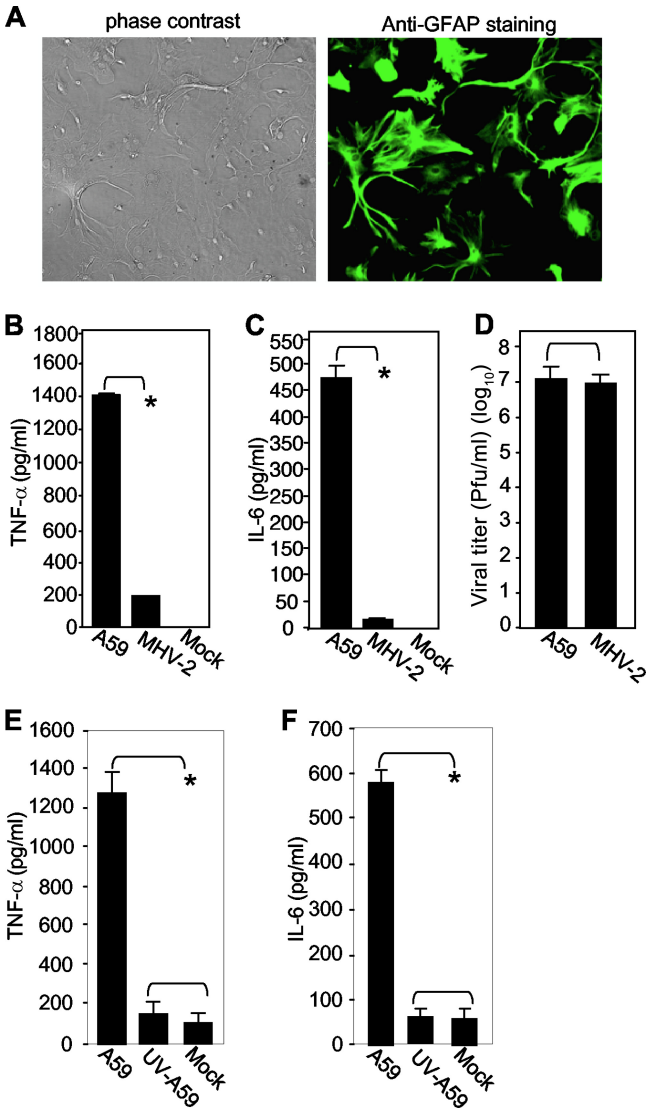

FIG. 1. Differential induction of TNF-α and IL-6 in primary mouse astrocytes by infection with MHV-A59 and MHV-2. (A) (Right) The purity of isolated primary mouse astrocytes was determined by immunofluorescence staining with an antibody specific for GFAP. (Left) Phase-contrast image showing the same field as in fluorescence staining. (B and C) Induction of TNF-α (B) and IL-6 (C) in primary astrocytes by MHV infection. Cells were infected with MHV-A59 or MHV-2 at an MOI of 5 or mock infected as a control. The culture supernatants were collected at 24 h p.i. The amounts of TNF-α (B) and IL-6 (C) proteins in the supernatants were determined using ELISA kits. The results are expressed as the mean number of picograms per milliliter for three independent experiments. The error bars indicate standard deviations of the means. The asterisks indicate the statistical significance between the pairs ($P < 0.05$). (D) Virus production in primary mouse astrocytes. Virus infection was carried out as for panels B and C, and virus titers were determined at 24 h p.i. by plaque assay on DBT cells. The results are expressed as the mean number of PFU per milliliter for three independent experiments. The error bars indicate standard deviations of the means. (E and F) Dependence of TNF-α and IL-6 induction on virus replication. Primary astrocytes were infected with live or UV-inactivated MHV-A59 at an MOI of 5 or mock infected. At 24 h p.i., the culture supernatants were collected to determine TNF-α (E) or IL-6 (F) protein amounts by ELISA as for panels B and C.

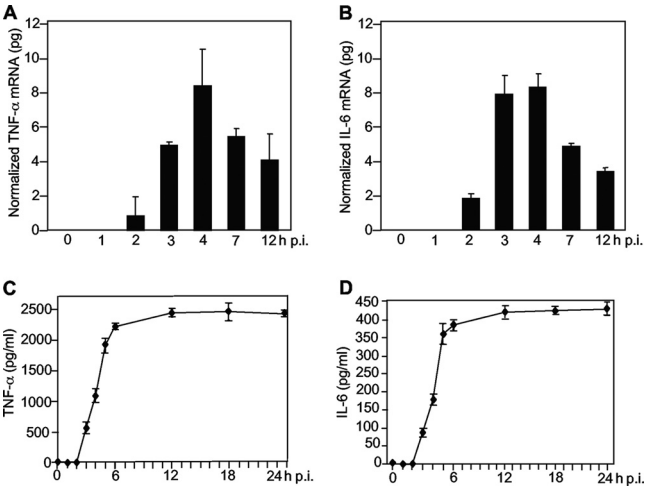

FIG. 2. Kinetics of induction of TNF-α and IL-6 in primary astrocytes by MHV-A59. Primary astrocytes were infected with MHV-A59 at an MOI of 5. The cells and culture medium were separately collected at 0, 1, 2, 3, 4, 7, and 12 h p.i. for mRNA (A and B) and protein (C and D) detection. (A and B) Kinetics of TNF-α and IL-6 mRNA induction. Intracellular RNAs were isolated, and the amounts of TNF-α and IL-6 mRNA were determined by qRT-PCR. The results are expressed as the mean number of picograms of cDNA normalized to β-actin for three independent experiments. The error bars indicate standard deviations of the means. (C and D) Kinetics of TNF-α and IL-6 protein induction. The amounts of TNF-α and IL-6 protein in the supernatants were determined with an ELISA kit. The results are expressed as the mean number of picograms per milliliter for three independent experiments. The error bars indicate standard deviations of the means.

were left. These data indicate that TNF-α and IL-6 mRNAs were rapidly induced by viral infection but that their turnover was rapid, as well. Like the induction of mRNA, the protein levels for TNF-α and IL-6 were detectable as early as 3 h p.i. and reached a plateau at 12 h p.i. However, unlike mRNAs, TNF-α and IL-6 proteins remained stable at a high level well beyond 24 h p.i. Taken together, these results demonstrate that TNF-α and IL-6 are induced by MHV infection, most likely at the transcription level, and that their inductions occur during the early stages of the virus life cycle.

Characterization of the signal transduction pathways involved in TNF-α and IL-6 induction by MHV infection. As described in the introduction, the activation of TNF-α and IL-6 can be triggered through all three MAP kinase signal transduction pathways, depending on the cell types and stimuli. It is not known which signaling pathway(s) is triggered by MHV infection to induce TNF-α and IL-6 expression in astrocytes. Therefore, primary astrocytes were treated with the p38 inhibitor SB203580 (20 μM) and its nonspecific control inhibitor SB202474 (20 μM), the JNK inhibitor SP600125 (40 μM), or the MEK inhibitor UO126 (50 μM) and its nonspecific control inhibitor UO124 (50 μM) for 1 h prior to and during virus infection. Mock-infected cells were used as a negative control. At 24 h p.i., the culture medium was collected and the protein levels for TNF-α and IL-6 were determined by ELISA. As shown in Fig. 3A and B, the JNK inhibitor SP600125 significantly blocked the induction of TNF-α and IL-6 by infection with MHV-A59, whereas both p38 and MEK inhibitors and

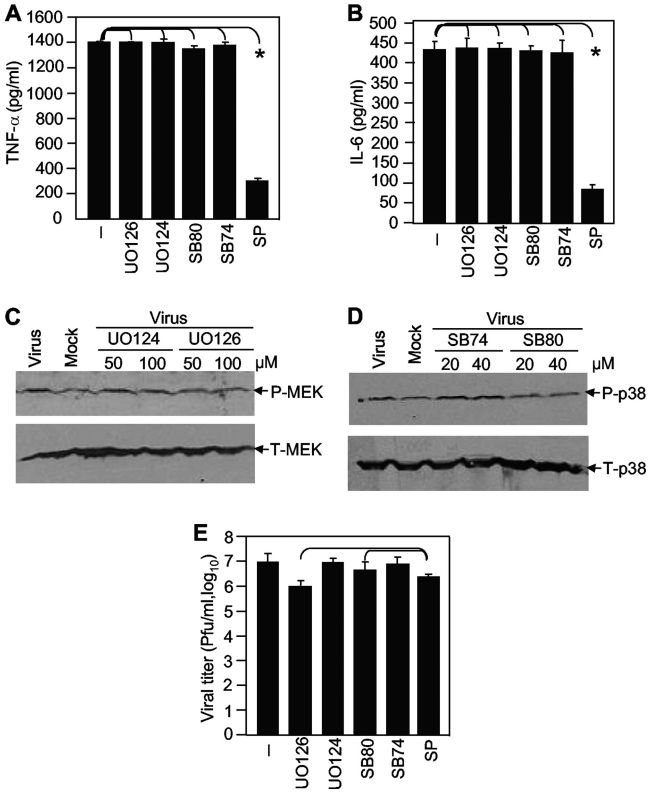

FIG. 3. Characterization of signaling pathways involved in TNF-α and IL-6 induction by MHV-A59 infection. (A and B) Primary astrocytes were treated with the MEK inhibitor UO126 (50 μM), the control inhibitor UO124 (50 μM), the p38 inhibitor SB203580 (20 μM), the control inhibitor SB202474 (20 μM), or the JNK inhibitor SP600125 (40 μM) or mock treated with dimethyl sulfoxide (−) for 1 h prior to and throughout infection. The cells were infected with MHV-A59 at an MOI of 5. The culture supernatants were collected at 24 h p.i. to determine TNF-α (A) and IL-6 (B) amounts and the virus titer (E). The amounts of TNF-α and IL-6 proteins were determined with an ELISA kit. The results are expressed as the mean number of picograms per milliliter for three independent experiments. The error bars indicate standard deviations of the means. The asterisks indicate statistical significance between the pairs ($P < 0.05$). (C and D) Effects of specific MAP inhibitors on MEK and p38 signaling. Primary astrocytes were treated with UO126/UO124 or SB203580 (SB80)/SB202474 (SB74) at the indicated concentrations and were infected with MHV-A59 at an MOI of 5. The cell lysates were used for detection of total (T) or phosphorylated (P) MEK and p38 in Western blots using specific antibodies. Cells infected with virus alone (lanes Virus) were used as a positive control for potential activation of the MAP kinase signaling pathways, while uninfected and untreated cells were used as a negative control for basal-level expression (lane Mock). (E) Virus titers were determined by virus plaque assay on DBT cells and are expressed as the mean number of PFU per milliliter for three independent experiments. The error bars indicate standard deviations of the means.

their nonspecific control inhibitors had no effect on TNF-α and IL-6 induction. These results indicate that the induction of TNF-α and IL-6 in astrocytes by MHV-A59 infection is mediated via the JNK signaling pathway, but not the p38 and MEK signaling pathways. In addition, although MHV-2 induced TNF-α at a very low level, the pattern of inhibition by the three MAP kinase inhibitors was very similar to that in MHV-A59-infected cells, suggesting that the activation pathways for the two viruses are similar (data not shown).

To confirm that the failure of p38 and MEK inhibitors (SB203580 and UO126) to block TNF-α and IL-6 expression was not due to their inability to inhibit the specific signaling pathways or to ineffective concentrations, primary astrocytes were treated with the specific and nonspecific inhibitors at the same or double concentrations and infected with MHV-A59 at the same MOI of 5. At 8 h p.i., the cell lysates were isolated and the protein levels for p38 and MEK were determined by Western blot analysis. As shown in Fig. 3C, phosphorylated MEK was slightly increased in virus-infected cells compared to that in mock-infected cells, suggesting an activation of the MEK signaling pathway by MHV infection. Treatment of cells with the specific inhibitor UO126 at both concentrations reduced the phosphorylated MEK to the background level, while treatment with the nonspecific inhibitor UO124 at the same concentrations did not have any effect on MEK phosphorylation. The total MEK protein levels remained similar in the experimental and control samples. Similarly, phosphorylated p38 was slightly increased in virus-infected cells compared to that in mock-infected cells. Treatment of cells with the specific inhibitor SB203580 completely blocked virus-induced phosphorylation of p38, while the nonspecific control inhibitor SB202474 had no effect on p38 phosphorylation (Fig. 3D). These data combined demonstrate that although the specific MEK and p38 inhibitors completely blocked virus-induced activation of the respective signaling pathways, they were unable to inhibit the induction of TNF-α and IL-6 by virus infection, thus establishing that induction of TNF-α and IL-6 by MHV infection in primary astrocytes is independent of the p38 and MEK signaling pathways.

We previously reported that the MEK inhibitor UO126 inhibited the replication of another MHV strain, JHM (3). To rule out the possibility that inhibition of TNF-α and IL-6 induction by the JNK inhibitor SP600125 might result from greater inhibition of virus replication than with the other two inhibitors, we also determined the virus titers in inhibitor-treated culture medium. While all three specific inhibitors inhibited virus production by 0.5 to 1 $\log_{10}$ PFU/ml, with the greatest inhibitory effect observed for UO126 (1 $\log_{10}$) (Fig. 3E), the differences in virus titers among the three inhibitor-treated cultures were statistically insignificant ($P > 0.05$). As expected, the nonspecific control inhibitors UO124 and SB202474 had no effect on virus titers (Fig. 3E). Thus, although all three MAP kinase pathways are able to regulate TNF-α and IL-6 induction by certain stimuli, MHV-induced TNF-α and IL-6 production is mediated specifically and exclusively through the JNK signaling pathway.

Differential activation of the JNK signaling pathway in primary astrocytes by MHV-A59 and MHV-2. The results described above indicate that the JNK signaling pathway might be activated by MHV infection. To test this possibility, we infected primary astrocytes with MHV-A59 and MHV-2 at an MOI of 5 or mock infected them as a control. Cells were collected at 24 h p.i. to determine the phosphorylation status of JNK and its substrate transcription factor c-Jun by Western blot analysis. As shown in Fig. 4A, the amounts of total JNK were similar in cells either infected with MHV-A59 and MHV-2 or mock infected, indicating that MHV infection did

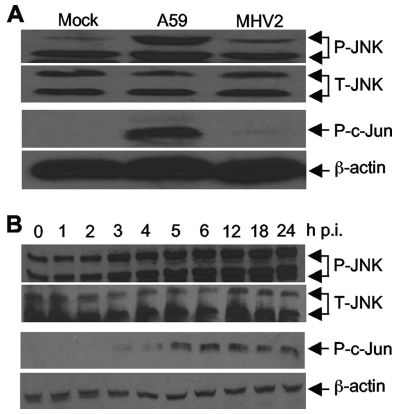

FIG. 4. Differential activation of the JNK signaling pathway by infections with MHV-A59 and MHV-2. (A) Primary astrocytes were infected with MHV-A59 or MHV-2 at an MOI of 5 or mock infected. Cells were then collected at 24 h p.i. Phosphorylated (P) and total (T) JNK and phosphorylated c-Jun were detected by Western blotting with phosphorylation-specific antibodies. β-Actin was used as an internal control. (B) Kinetics of JNK pathway activation by MHV-A59 infection. Primary astrocytes were infected with MHV-A59 at an MOI of 5. The cell lysates were collected at 0, 1, 2, 3, 4, 5, 6, 12, 18, and 24 h p.i. Phosphorylated and total JNK and phosphorylated c-Jun were detected by Western blotting as for panel A.

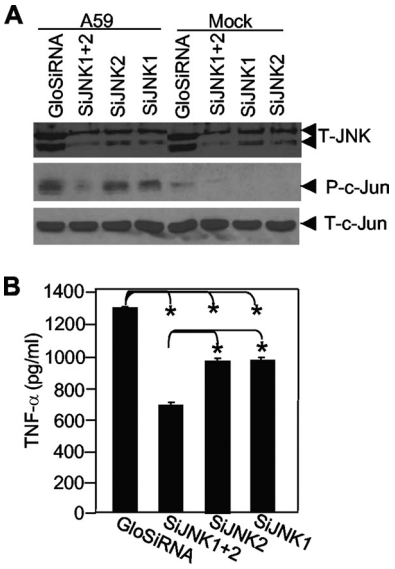

FIG. 5. TNF-α induction by MHV-A59 infection is inhibited by JNK siRNAs. (A) Primary astrocytes were transfected with siRNAs to JNK1 and JNK2 singly or in combination or were transfected with a nonspecific siRNA (GloSiRNA). The cells were then infected with MHV-A59 at an MOI of 5 or mock infected. The cell lysates were collected at 24 h p.i. for detection of JNK, phosphorylated (P) c-Jun, and total (T) c-Jun by Western blotting using the respective antibodies. (B) Culture supernatants were collected at 24 h p.i. for detection of TNF-α protein by ELISA. The results are expressed as the mean number of picograms per milliliter for three independent experiments. The error bars indicate standard deviations of the means. The asterisks indicate a statistical significance between the pairs ($P < 0.05$).

not activate JNK at the transcriptional and translational levels. Interestingly, although the amounts of one of the two phosphorylated JNK species (with a lower molecular weight) were similar in MHV-infected and mock-infected cells, the amount of the other phosphorylated JNK species was significantly increased in MHV-A59-infected cells. The amount of the phosphorylated JNK species with a higher molecular weight in MHV-2-infected cells was slightly more than that in mock-infected cells. These results demonstrate that the JNK signaling pathway is differentially activated in astrocytes by MHV-A59 and MHV-2, which is correlated with the differential induction of TNF-α and IL-6 by the two viruses. The results also suggest that the activation of the JNK pathway is likely mediated through a specific phosphorylation site on JNK, which leads to the detection of the species with a higher molecular weight. To further establish that the JNK signaling pathway is indeed activated, we determined the phosphorylation status of its substrate, c-Jun. Indeed, we detected a significant amount of phosphorylated c-Jun in MHV-A59-infected cells but very little in MHV-2- and mock-infected cells, thus establishing that the JNK signaling pathway is differentially activated by MHV infections.

To provide further evidence for the signaling activation, we determined the kinetics of JNK and c-Jun phosphorylation following MHV-A59 infection. We found that both phosphorylated JNK and phosphorylated c-Jun were readily detectable at 2 to 3 h p.i. (Fig. 4B). Thus, the kinetics of JNK signaling pathway activation and TNF-α induction by MHV infection were similar, suggesting a potential link between the signaling events.

Knockdown of JNK by JNK-specific small interfering RNAs (siRNAs) inhibited TNF-α induction by MHV-A59 infection. To establish that the activation of the JNK signaling pathway is directly linked to TNF-α induction by MHV infection, we transfected primary astrocytes with siRNAs specific for JNK1 or JNK2 individually or in combination. Nonspecific siRNA with green fluorescence was used as a negative control and for monitoring the transfection efficiency, which reached more than 90% (data not shown). At 36 h posttransfection, cells were infected with MHV-A59 at an MOI of 5 or mock infected. At 24 h p.i., cells were collected to determine the effectiveness of JNK knockdown by siRNAs by Western blot analysis, while the supernatants were used for determining TNF-α protein levels by ELISA. The results showed that there was a significant inhibition of total JNK in MHV-A59-infected cells when both JNK siRNAs were transfected but only slight inhibition when JNK1 and JNK2 siRNAs were transfected individually (Fig. 5A, top). To further assess the functional significance of the JNK pathway inhibition by the siRNAs, we also determined the effect on the JNK substrate, c-Jun. Indeed, phosphorylated c-Jun was significantly inhibited when both siRNAs were transfected together (Fig. 5A, middle). Phosphorylated c-Jun levels were significantly higher in virus-infected cells than in mock-infected cells (Fig. 5A, middle), consistent with the activation of the JNK pathway by virus infection (Fig. 4). However, transfection with the nonspecific and JNK-specific siRNAs did not alter the expression level of total c-Jun (Fig. 5A, bottom), indicating that reduction of phosphorylated c-Jun is a consequence of the inhibition of its upstream kinase JNK protein by the siRNAs and not inhibition of the c-Jun protein level. We then determined whether knockdown of JNK by siRNAs would affect TNF-α induction. We

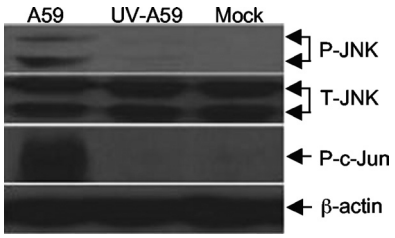

FIG. 6. Virus replication is required for JNK activation. Primary astrocytes were infected with live or UV-inactivated MHV-A59 at an MOI of 5 or mock infected. At 24 h p.i., the cell lysates were isolated and used for detecting phosphorylated JNK (P-JNK) and c-Jun (P-c-Jun) or total JNK (T-JNK) by Western blot analysis using specific antibodies as described in the legend to Fig. 5. β-Actin was used as an internal control.

determined the amounts of TNF-α in culture supernatants that were transfected with the siRNAs for 36 h and then infected with MHV-A59 for 24 h. The results showed that transfection of the JNK siRNAs significantly inhibited TNF-α production and that the inhibitory effect was greater in cells transfected with both siRNAs than in cells transfected with the siRNAs individually (Fig. 5B). Combined with the results obtained with the JNK inhibitor SP600125 (Fig. 3), these data thus establish that induction of TNF-α by MHV infection is mediated through the activation of the JNK signaling pathway.

Virus replication is required for activation of the JNK signaling pathway. As shown in Fig. 1, virus replication is required for TNF-α and IL-6 induction. To further establish the cause-effect relationship, we determined whether activation of the JNK signaling pathway also requires virus replication. Astrocytes were infected with MHV-A59 at an MOI of 5 or with UV-inactivated MHV-59 at an equivalent preinactivation titer. The completeness of UV inactivation was confirmed by plaque assay. Cell lysates were collected at 24 h p.i., and the phosphorylation status of both JNK and c-Jun was determined by Western bloting with specific antibodies. As expected, UV-inactivated MHV-A59 did not activate JNK and c-Jun phosphorylation (Fig. 6), indicating that activation of the JNK signaling pathway requires virus replication. This finding further supports the conclusion that induction of TNF-α by MHV infection is mediated via the activation of the JNK signaling pathway.

NF-κB is activated by MHV infection. Since the promoter of the TNF-α gene contains four NF-κB binding sites (Fig. 7A) and activation of NF-κB can induce the expression of proinflammatory cytokines, including TNF-α and IL-6, in many types of cells (5, 29), we wondered if MHV-A59 infection could activate NF-κB. Primary astrocytes were infected with MHV-A59 at an MOI of 5 or mock infected. At 8 h p.i., the nuclear translocation of NF-κB was monitored following immunofluorescence staining and observed under a confocal laser scanning microscope. Indeed, we observed that nuclear translocation of NF-κB was detected in a significant number of virus-infected cells (Fig. 7B, right) compared with mock-infected cells, which had little nuclear translocation (Fig. 7B, left). To verify this finding, cell nuclear extracts were isolated and NF-κB activity was determined with the commercial TransAM NF-κB p65 kit, which measures the binding capacity of NF-κB from the nuclear extracts to the consensus binding

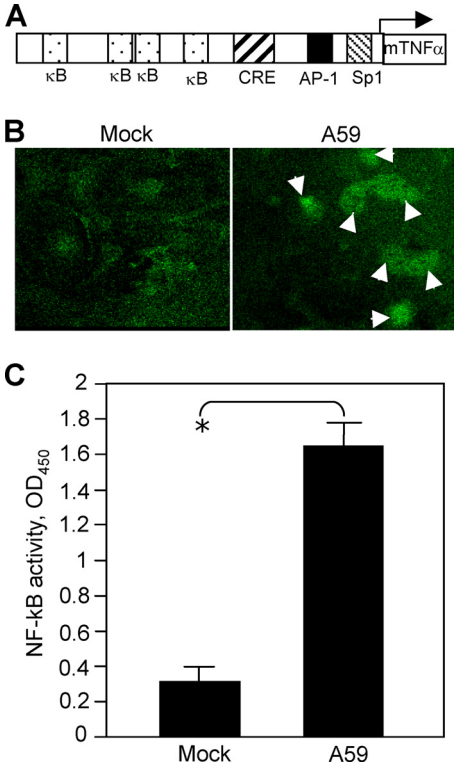

FIG. 7. Activation of TNF-α by MHV-A59 infection. (A) Schematic diagram showing the sequence elements of the murine TNF-α (mTNF-α) promoter and the binding sites for transcription factors NF-κB (κB), CRE, AP-1, and Sp1. (B) Nuclear translocation of NF-κB following MHV-A59 infection. Cells were infected with MHV-A59 at an MOI of 5 for 18 h (right) or mock infected (left). The cells were fixed with 4% paraformaldehyde and stained with primary anti-NF-κB p65 polyclonal antibody and fluorescein isothiocyanate-conjugated goat anti-rabbit antibody. The images were taken with a digital camera under a fluorescence microscope. The arrows indicate the nuclear translocation. (C) Assay for NF-κB activation. Primary astrocytes were infected with MHV-A59 at an MOI of 5 or mock infected. At 18 h p.i., nuclear extracts were isolated and NF-κB activity was determined with the TransAM NF-κB p65 kit as described in Materials and Methods. The results are expressed as the mean absorbance at 450 nm (OD_{450}) for three independent experiments. The error bars indicate standard deviations of the mean. The asterisk indicates statistical significance between the pair ($P < 0.05$).

sequence. The results showed that MHV-A59 infection activated NF-κB (Fig. 7C).

MHV-induced NF-κB activation is mediated through the JNK signaling pathway. To determine how NF-κB is activated by MHV infection, we treated cells with NF-κB inhibitors in the presence or absence of the JNK inhibitors. At 24 h p.i., cell nuclear extracts were isolated and NF-κB activity was determined with the same TransAM NF-κB p65 assay kit. We found that treatment of cells with the JNK inhibitor SP600125 significantly inhibited the NF-κB activity to a level comparable with that obtained with the NF-κB p65-inhibitory peptide (Fig. 8). However, a combination treatment with the NF-κB-inhibitory peptide (Ser276) and the JNK inhibitor SP600125 did not result in further inhibition of NF-κB activity, suggesting that it is unlikely that additional pathways activated NF-κB during virus infection. In contrast, treatment with a nonspecific pep-

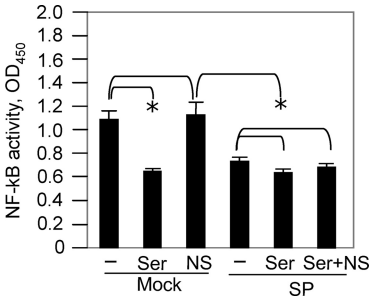

FIG. 8. MHV-induced NF-κB activation is mediated through the JNK signaling pathway. Primary astrocytes were pretreated with the NF-κB inhibitor peptide Ser276 (Ser) at 50 μM or with a nonspecific inhibitor (NS) or were untreated (−) in the presence (SP) or absence (mock) of the JNK inhibitor SP600125. The cells were then infected with MHV-A59 at an MOI of 5. At 24 h p.i., cell nuclear extracts were prepared and NF-κB activity was determined with the TransAM NF-κB p65 assay kit, as described in Materials and Methods. The results are expressed as the mean absorbance at 450 nm (OD_{450}) for three independent experiments. The error bars indicate standard deviations of the mean. The asterisks indicate statistical significance between the pairs ($P < 0.05$).

tide did not inhibit NF-κB activity. Thus, these results indicate that MHV-induced NF-κB activation is likely mediated through the actions of the JNK signaling pathway.

Role of NF-κB activation in TNF-α and IL-6 induction by MHV infection. To determine if NF-κB plays a role in TNF-α and IL-6 induction, we employed a complementary approach using two different NF-κB inhibitors. It has been reported that the NF-κB-inhibitory peptide SC3060 blocks the nuclear translocation of NF-κB while the NF-κB p65 (Ser276)-inhibitory peptide blocks the binding of the NF-κB p65 subunit to its consensus binding site, thereby inhibiting downstream gene transcription (2, 32, 44). Primary astrocytes were treated with both NF-κB inhibitors or with a nonspecific peptide and were infected with MHV-A59. Cell lysates were collected for determination of the activity of the NF-κB complex with a commercial TransAM NF-κB p65 kit. The results showed that MHV-A59 infection activated NF-κB and that treatment of cells with both NF-κB inhibitors significantly inhibited NF-κB activity ($P < 0.05$) (Fig. 9A). In contrast, NF-κB activity was not inhibited when the cells were treated with the nonspecific inhibitor (Fig. 9A). However, treatment of cells with these inhibitors did not significantly inhibit TNF-α and IL-6 induction by virus infection (Fig. 9B and C). Thus, the precise role of NF-κB in TNF-α and IL-6 induction remains unclear (see Discussion).

MHV S and N genes are not responsible for the differential induction of TNF-α and IL-6 in astrocytes. The S protein of MHV has been shown to be an important determinant of pathogenicity in mice (9), and the N protein is a potential transcription factor that activates liver prothrombinase gene expression, which can contribute to MHV-induced fulminant hepatitis in mice (28). In an attempt to identify which viral gene(s) is potentially responsible for the differential induction of proinflammatory cytokines in astrocytes, we used two recombinant viruses (Penn-98-1 and icA59/2N) whose S or N gene was replaced with the counterpart from MHV-2 (Fig. 10A). The growth properties of the two recombinant viruses

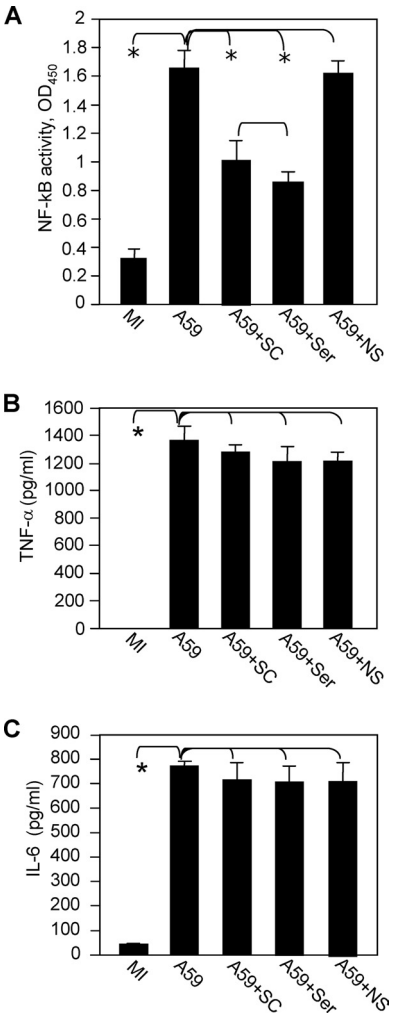

FIG. 9. Role of NF-κB activation in the induction of TNF-α and IL-6 in primary astrocytes by MHV infection. (A) Primary astrocytes were pretreated with the NF-κB inhibitor SC3060 or NF-κB p65 (Ser276)-inhibitory peptide at a concentration of 50 μM or treated with a control peptide (NS). The cells were then infected with MHV-A59 at an MOI of 5 or mock infected (MI) as a control. The cell nuclear lysates were extracted at 24 h p.i. for determination of NF-κB activity with a TransAM NF-κB p65 kit. (B and C) NF-κB activity was expressed as the mean absorbance at 450 nm (OD_{450}) in three independent experiments. The error bars indicate standard deviations of the means. The culture supernatants were collected at 24 h p.i. to measure TNF-α (B) and IL-6 (C) protein levels by ELISA. The amounts of TNF-α and IL-6 were expressed as mean numbers of picograms per milliliter in three independent experiments. The error bars indicate standard deviations of the means. The asterisks indicate statistical significance between the pairs ($P < 0.05$).

were similar to those of the wild-type MHV-A59 and MHV-2 in primary astrocytes (data not shown). Following infection of primary astrocytes with the wild-type and recombinant MHVs for 24 h, the protein levels of TNF-α and IL-6 in the culture supernatants were determined by ELISA. The results showed that both recombinant viruses induced TNF-α and IL-6 to levels similar to those induced by the wild-type MHV-A59 (Fig. 10B and C), indicating that viral genes other than the S and N genes are responsible for the induction of TNF-α and IL-6 in astrocytes by MHV-A59 infection.

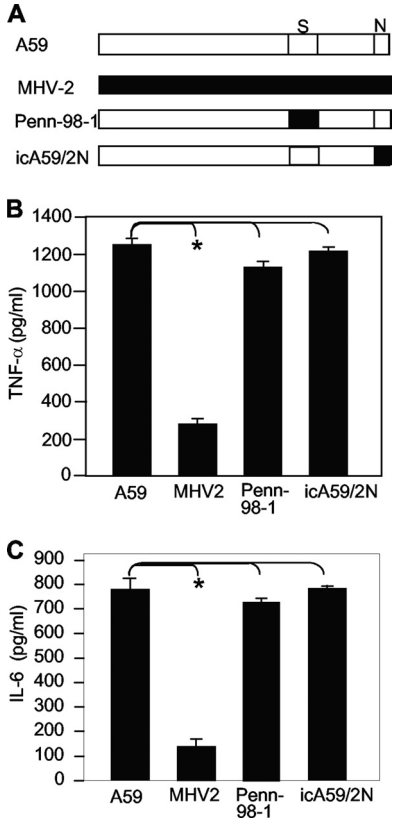

FIG. 10. The S and N genes of MHV-A59 are not responsible for the induction of TNF-α. (A) Schematic diagram of the MHV genome highlighting the differences in S and N genes in the recombinants Penn-98-1 and icA59/2N with respect to the parental MHV-A59 and MHV-2. (B and C) Induction of TNF-α and IL-6 in primary astrocytes by MHV infection. Primary astrocytes were infected with the recombinant viruses Penn-98-1 and icA59/2N or the parental viruses MHV-A59 and MHV-2 at an MOI of 5, and the cell culture supernatants were collected at 24 h p.i. The protein levels of TNF-α and IL-6 were determined by ELISA and are expressed as mean numbers of picograms per milliliter in three independent experiments. The error bars indicate standard deviations of the means. The asterisks indicate statistical significance between the pairs ($P < 0.05$).

DISCUSSION

In the present study, we demonstrated that induction of TNF-α expression in primary mouse astrocytes by MHV-A59 infection is mediated specifically through activation of the JNK signaling pathway. This conclusion was drawn from initial observations that TNF-α expression was inhibited only by an inhibitor specific for JNK, but not by those specific for p38 and MEK (Fig. 3). It was further confirmed by using siRNAs specific for JNK (Fig. 4 and 5). It is worth noting that although a substantial level of TNF-α production was detected even after siRNA-mediated knockdown of JNK (Fig. 5), it was likely due to incomplete knockdown of JNK by specific siRNAs, which is strongly activated by MHV infection (Fig. 5). Thus, although TNF-α expression can be regulated by all three MAP kinase signaling pathways (6, 20), MHV-induced TNF-α expression is specifically and exclusively regulated via the JNK signaling pathway. Indeed, both JNK and its substrate transcription factor c-Jun are activated in MHV-A59-infected astrocytes (Fig. 4). Interestingly, although both JNK species are significantly phosphorylated in MHV-A59-infected cells, only the larger JNK species likely plays a role in TNF-α induction, since significant levels of phosphorylation of the smaller JNK species were also detected in MHV-2- and mock-infected cells (Fig. 4). These results suggest that unlike other stimuli, MHV-A59 infection induces TNF-α expression in primary astrocytes through the activation of a distinct species or phosphorylation site in JNK. To our knowledge, this phenomenon has not been described before.

The promoter region of TNF-α contains four NF-κB binding sites, a calcium- and cyclic-AMP-responsive element (CRE), and an AP-1 and Sp1 *cis*-binding site (5). Thus, expression of TNF-α at the transcriptional level is regulated by multiple transcriptional factors individually or in combination, depending on the cell type and stimulus (10, 22, 27, 29, 33). While the basal transcription of TNF-α is controlled by Sp1, inducible expression of TNF-α is likely regulated by NF-κB, cyclic AMP, and AP-1. Our finding that MHV-induced TNF-α expression is mediated through activation of the JNK/c-Jun signaling pathway suggests that transcription of the TNF-α gene is induced by c-Jun upon binding directly to the AP-1 binding site or, in coordination with other factors, to the CRE site in the promoter. It has been shown that both AP-1 and CREs can functionally cooperate or work independently (45, 46). C-Jun interacts with another transcription factor, NFATp, to regulate TNF-α expression in activated T cells by binding of two NFATp molecules to the kappa 3 element in association with c-Jun binding to an immediately adjacent CRE site (45, 46). Alternatively, the activation of JNK may also activate other downstream transcription factors, such as NF-κB, which in turn induces expression of TNF-α through binding to the four NF-κB consensus binding sites in the TNF-α promoter. We examined the latter possibility by determining the activation and nuclear translocation of NF-κB following MHV-A59 infection. Our data show that NF-κB is indeed activated by MHV infection and that its activation is dependent on the activation of the JNK signaling pathway (Fig. 7 and 8). However, it appears that activation and nuclear translocation of NF-κB do not play critical roles in TNF-α and IL-6 induction, since inhibition of NF-κB activation and blockage of nuclear translocation by specific peptide inhibitors do not significantly affect TNF-α and IL-6 expression following MHV-A59 infection (Fig. 9 and data not shown). One possible explanation is that c-Jun is immediately and drastically activated by MHV infection and that c-Jun plays a predominant role in inducing TNF-α/IL-6 expression under such conditions. Another possibility is that NF-κB may be activated at later stages of virus infection or secondarily by secreted TNF-α. Consequently, inhibition of NF-κB activation has little effect on initial TNF-α/IL-6 induction. It should be noted that the precise kinetics of NF-κB activation was not determined in the current study. A third possibility is that the level of NF-κB activation may not be proportional to the level of cytokine production. As a result, a 40 to 50% reduction in NF-κB activity by the inhibitors may not be sufficient to significantly inhibit TNF-α and IL-6 induction (Fig. 9). Alternatively, while these peptide inhibitors appear to be specific for the canonical NF-κB pathway, MHV-induced NF-κB activation may utilize noncanonical pathways. As a result, these inhibitors cannot block NF-κB-dependent

TNF-α and IL-6 induction (26). Irrespective of its role in regulating TNF-α expression, activation of NF-κB in MHV-infected astrocytes likely has profound effects on host cells, since NF-κB is a key transcription factor that regulates the transcription of a wide array of cellular genes, which are involved in homeostasis, development, differentiation, host defense, or induction of inflammation. Thus, activation of NF-κB may play important roles in the pathogenesis of MHV-induced CNS diseases. Such potential roles for NF-κB will be examined in the future. Nevertheless, our data unequivocally establish that MHV-induced expression of TNF-α is mediated through activation of the JNK signaling pathway.

In an attempt to identify the potential viral gene(s) responsible for the differential induction of proinflammatory cytokines, we used two chimeric viruses with an exchange of the S or N gene between MHV-A59 and MHV-2 and found that neither the S nor the N protein is responsible for differential TNF-α and IL-6 induction (Fig. 10). Thus, it remains unclear what other viral gene(s) is responsible for TNF-α and IL-6 induction. Our studies of the kinetics of TNF-α expression at both mRNA and protein levels showed that TNF-α is readily induced in virus-infected astrocytes as early as 2 h p.i. (Fig. 2), which suggests that TNF-α induction is likely mediated during early stages of the virus life cycle, including viral entry and viral protein and RNA synthesis. However, because viral entry, which is largely mediated through the S protein, cannot account for the TNF-α induction, viral genome translation and RNA synthesis, which usually take place during the first hours following viral entry, are most likely to be the trigger. Consistent with this interpretation is the finding that infection with UV-inactivated MHV-A59 failed to induce TNF-α expression or to activate the JNK signaling pathway (Fig. 1 and 6). Thus, induction of TNF-α requires virus replication. To further determine whether the protein products resulted from genome translation or whether the viral mRNAs following replication induced TNF-α, we treated primary astrocytes with cycloheximide prior to and during virus infection. Unfortunately, treatment with cycloheximide alone (without virus infection) induced a significant amount of TNF-α secretion into the culture medium (data not shown). Thus, we were unable to precisely determine the viral factors involved in differential TNF-α and IL-6 induction. Future experiments should address this important question.

ACKNOWLEDGMENTS

We thank Ehud Lavi (University of Pennsylvania School of Medicine, Philadelphia) for kindly providing the recombinant virus Penn-98-1.

This work was supported by Public Health Service grant NS047499 and in part by the P30 core grant NS047546 and grant AI061204 from the National Institutes of Health.

REFERENCES

1. **Buchmeier, M. J., H. A. Lewicki, and P. J. Talbot.** 1984. Murine hepatitis virus-4 (strain JHM)-induced neurologic disease is modulated in vivo by monoclonal antibody. Virology **132:**261–270.
2. **Bylund, J., K. L. MacDonald, K. L. Brown, P. Mydel, L. V. Collins, R. E. W. Hancock, and D. P. Speert.** 2007. Enhanced inflammatory responses of chronic granulomatous disease leukocytes involve ROS-independent activation of NF-κB. Eur. J. Immunol. **37:**1087–1096.
3. **Cai, Y., Y. Liu, and X. Zhang.** 2007. Suppression of coronavirus replication by inhibition of the MEK signaling pathway. J. Virol. **81:**446–456.
4. **Chung, I. Y., J. Kwon, and E. N. Benveniste.** 1992. Role of protein kinase C activity in tumor necrosis factor-alpha gene expression. Involvement at the transcriptional level. J. Immunol. **149:**3894–3902.
5. **Collart, M. A., P. Baeuerle, and P. Vassalli.** 1990. Regulation of tumor necrosis factor transcription in macrophages: involvement of four B-like motifs and of constitutive and inducible forms of NF-B. Mol. Cell. Biol. **10:**1498–1506.
6. **Csonga, R., E. E. Prieschl, D. Jaksche, V. Novotny, and T. Baumruker.** 1998. Common and distinct signaling pathways mediate the induction of TNF-alpha and IL-5 in IgE plus antigen-stimulated mast cells. J. Immunol. **160:** 273–283.
7. **Dalziel, R. G., P. W. Lampert, P. J. Talbot, and M. J. Buchmeier.** 1986. Site-specific alteration of murine hepatitis virus type 4 peplomer glycoprotein E2 results in reduced neurovirulence. J. Virol. **59:**463–471.
8. **Das Sarma, J., L. Fu, S. T. Hingley, and E. Lavi.** 2001. Mouse hepatitis virus type-2 infection in mice: an experimental model system of acute meningitis and hepatitis. Exp. Mol. Pathol. **1:**1–12.
9. **Das Sarma, J., L. Fu, J. C. Tsai, S. R. Weiss, and E. Lavi.** 2000. Demyelination determinants map to the spike glycoprotein gene of coronavirus mouse hepatitis virus. J. Virol. **74:**9206–9213.
10. **Economou, J. D., K. Rhoades, R. Essner, W. H. McBride, J. C. Gasson, and D. L. Morton.** 1989. Genetic analysis of the human tumor necrosis factor α/cachectin promoter region in a macrophage cell line. J. Exp. Med. **170:** 321–326.
11. **Fisher, S. N., Y. U. Kim, and M. L. Shin.** 1994. Tyrosine kinase activation by Newcastle disease virus is required for TNF-alpha gene induction in astrocytes. J. Immunol. **153:**3210–3217.
12. **Hirano, N., K. Fujiwara, S. Hino, and M. Matumoto.** 1974. Replication and plaque formation of mouse hepatitis virus (MHV-2) in mouse cell line DBT culture. Arch. Gesamte Virusforsch. **44:**298–302.
13. **Hirano, N., T. Murakami, F. Taguchi, K. Fujiwara, and M. Matumoto.** 1981. Comparison of mouse hepatitis virus strains for pathogenicity in weanling mice infected by various routes. Arch. Virol. **70:**69–73.
14. **Kassiotis, G., M. Pasparakis, G. Kollias, and L. Probert.** 1999. TNF accelerates the onset but does not alter the incidence and severity of myelin basic protein-induced experimental autoimmune encephalomyelitis. Eur. J. Immunol. **29:**774–780.
15. **Klinkert, W. E. F., K. Kojima, W. Lesslauer, W. Rinner, H. Lassmann, and H. Wekerle.** 1994. TNF-α receptor fusion protein prevents experimental autoimmune encephalomyelitis and demyelination in Lewis rats: an overview. J. Neuroimmunol. **72:**163–168.
16. **Knobler, R. L., M. V. Haspel, and M. B. Oldstone.** 1981. Mouse hepatitis virus type 4 (JHM strains)-induced fatal central nervous system disease. I. Genetic control and murine neuron as the susceptible site of disease. J. Exp. Med. **153:**832–843.
17. **Lane, T. E., V. C. Asensio, N. Yu, A. D. Paoletti, I. L. Campbell, and M. J. Buchmeier.** 1998. Dynamic regulation of alpha- and beta-chemokine expression in the central nervous system during mouse hepatitis virus-induced demyelinating disease. J. Immunol. **16:**970–978.
18. **Lavi, E., D. H. Gilden, M. K. Highkin, and S. R. Weiss.** 1986. The organ tropism of mouse hepatitis virus A59 in mice is dependent on dose and route of inoculation. Lab. Anim. Sci. **36:**130–135.
19. **Lavi, E., D. H. Gilden, Z. Wroblewska, L. B. Rorke, and S. R. Weiss.** 1984. Experimental demyelination produced by the A59 strain of mouse hepatitis virus. Neurology **34:**597–603.
20. **Lee, J. C., J. T. Laydon, P. C. McDonnell, T. F. Gallagher, S. Kumar, D. Green, D. McNulty, M. J. Blumenthal, J. R. Heys, and S. W. Landvatter.** 1994. A protein kinase involved in the regulation of inflammatory cytokine biosynthesis. Nature **372:**739–746.
21. **Lee, Y. B., J. W. Schrader, and S. U. Kim.** 2000. p38 MAP kinase regulates TNF-alpha production in human astrocytes and microglia by multiple mechanisms. Cytokine **12:**874–880.
22. **Leitman, D. C., R. C. Ribeiro, E. R. Mackow, J. D. Baxter, and B. L. West.** 1991. Identification of a tumor necrosis factor-responsive element in the tumor necrosis factor alpha gene. J. Biol. Chem. **266:**9343–9346.
23. **Li, Y., L. Fu, D. M. Gonzales, and E. Lavi.** 2004. Coronavirus neurovirulence correlates with the ability of the virus to induce proinflammatory cytokine signals from astrocytes and microglia. J. Virol. **78:**3398–3406.
24. **Lieberman, A. P., P. M. Pitha, H. S. Shin, and M. L. Shin.** 1989. Production of tumor necrosis factor and other cytokines by astrocytes stimulated with lipopolysaccharide or a neurotropic virus. Proc. Natl. Acad. Sci. USA **86:** 6348–6352.
25. **Lin, M. T., S. A. Stohlman, and D. R. Hinton.** 1997. Mouse hepatitis virus is cleared from the central nervous systems of mice lacking perforin-mediated cytolysis. J. Virol. **71:**383–391.
26. **Liu, H., P. Sidiropoulos, G. Song, L. J. Pagliari, M. J. Birrer, B. Stein, J. Anrather, and R. M. Pope.** 2000. TNF-α gene expression in macrophages: regulation by NF-κB is independent of c-Jun or C/EBP. J. Immunol. **164:** 4277–4285.
27. **Newell, C. L., A. B. Deisseroth, and G. Lopez-Berestein.** 1994. Interaction of nuclear proteins with an AP-1/CRE like promoter sequence in the human TNF-α gene. J. Leukoc. Biol. **56:**27–35.
28. **Ning, Q., M. Liu, P. Kongkham, M. M. Lai, P. A. Marsden, J. Tseng, B.**

Pereira, M. Belyavskyi, J. Leibowitz, M. J. Phillips, and G. Levy. 1999. The nucleocapsid protein of murine hepatitis virus type 3 induces transcription of the novel fgl2 prothrombinase gene. J. Biol. Chem. **274:**9930–9936.
29. **Paludan, S., S. Ellermann-Eriksen, V. Kruys, and S. C. Mogensen.** 2001. Expression of TNF-alpha by herpes simplex virus-infected macrophages is regulated by a dual mechanism: transcriptional regulation by NF-kappa B and activating transcription factor 2/Jun and translational regulation through the AU-rich region of the 3′ untranslated region. J. Immunol. **167:**2202–2208.
30. **Parra, B., D. R. Hinton, N. W. Marten, C. C. Bergmann, M. T. Lin, C. S. Yang, and S. A. Stohlman.** 1999. IFN-gamma is required for viral clearance from central nervous system oligodendroglia. J. Immunol. **162:**1641–1647.
31. **Pewe, L., and S. Perlman.** 2002. Cutting edge: CD8 T cell-mediated demyelination is IFN-gamma dependent in mice infected with a neurotropic coronavirus. J. Immunol. **168:**1547–1551.
32. **Ramana, K. V., R. Tammali, A. B. Reddy, A. Bhatnagar, and S. K. Srivastava.** 2007. Aldose reductase-regulated tumor necrosis factor alpha production is essential for high glucose-induced vascular smooth muscle cell growth. Endocrinology **148:**4371–4384.
33. **Rhoades, K. L., S. H. Golub, and J. S. Economou.** 1992. The regulation of human tumor necrosis factor α promoter region in macrophage, T cell, and B cell lines. J. Biol. Chem. **267:**22101–22107.
34. **Ruddle, N. H., C. M. Bergman, K. M. McGrath, E. G. Lingenheld, M. L. Grunnet, S. J. Padula, and R. B. Clark.** 1990. An antibody to lymphotoxin and tumor necrosis factor prevents transfer of experimental allergic encephalomyelitis. J. Exp. Med. **172:**1193–1200.
35. **Rudin, W., H. P. Eugster, G. Bordmann, J. Bonato, M. Muller, M. Yamage, and B. Ryffel.** 1997. Resistance to cerebral malaria in tumor necrosis factor-α/β deficient mice is associated with a reduction of intercellular adhesion molecule-1 up-regulation and T helper type 1 response. Am. J. Pathol. **150:**257–266.
36. **Saukkonen, K., S. Sande, C. Cioffe, S. Wolpe, B. Sherry, A. Cerami, and E. Tuomanen.** 1990. The role of cytokines in the generation of inflammation and tissue damage in experimental gram-positive meningitis. J. Exp. Med. **171:**439–448.
37. **Schwender, S., A. Hein, H. Imrich, S. Czub, and R. Dorries.** 1999. Modulation of acute coronavirus-induced encephalomyelitis in gamma-irradiated rats by transfer of naive lymphocyte subsets before infection. J. Neurovirol. **5:**249–257.
38. **Selmaj, K., C. S. Raine, and A. H. Cross.** 1991. Anti-tumor necrosis factor therapy abrogates autoimmune demyelination. Ann. Neurol. **30:**694–700.
39. **Sommer, N., P. A. Loschmann, G. H. Northoff, M. Weller, A. Steinbecher, J. P. Steinbach, R. Lichtenfels, R. Meyermann, R. Reitmuller, A. Fontana, J. Dichgans, and R. Martin.** 1995. The antidepressant Rolipram suppresses cytokine production and prevents autoimmune encephalomyelitis. Nat. Med. **1:**244–248.
40. **Spriggs, D. R., S. Deutsch, and D. W. Kufe.** 1992. Genomic structure, induction, and production of TNF-alpha. Immunol. Ser. **56:**3–34.
41. **Stohlman, S. A., C. C. Bergmann, R. C. Veen, and D. R. Hinton.** 1995. Mouse hepatitis virus-specific cytotoxic T lymphocytes protect from lethal infection without eliminating virus from the central nervous system. J. Virol. **69:**684–694.
42. **Stohlman, S. A., D. R. Hinton, D. Cua, E. Dimacali, J. Sensintaffar, F. M. Hofman, S. M. Tahara, and Q. Yao.** 1995. Tumor necrosis factor expression during mouse hepatitis virus-induced demyelinating encephalomyelitis. J. Virol. **69:**5898–5903.
43. **Sun, N., D. Grzybicki, R. F. Castro, S. Murphy, and S. Perlman.** 1995. Activation of astrocytes in the spinal cord of mice chronically infected with a neurotropic coronavirus. Virology **213:**482–493.
44. **Takada, Y., S. Singh, and B. B. Aggarwal.** 2004. Identification of a p65 peptide that selectively inhibits NF-κB activation induced by various inflammatory stimuli and its role in down-regulation of NF-κB-mediated gene expression and upregulation of apoptosis. J. Biol. Chem. **279:**15096–15104.
45. **Tsai, E. Y., J. Jain, P. A. Pesavento, A. Rao, and A. E. Goldfeld.** 1996. Tumor necrosis factor gene regulation in activated T cells involves ATF-2/Jun and NFATp. Mol. Cell. Biol. **16:**459–467.
46. **Tsai, E. Y., J. Yie, D. Thanos, and A. E. Goldfeld.** 1996. Cell-type-specific regulation of the human tumor necrosis factor gene in B cells and T cells by NFATp and ATF-2/JUN. Mol. Cell. Biol. **16:**5232–5244.
47. **Wege, H., J. R. Stephenson, M. Koga, H. Wege, and V. ter Meulen.** 1981. Genetic variation of neurotropic and non-neurotropic murine coronaviruses. J. Gen. Virol. **54:**67–74.
48. **Yount, B., M. R. Denison, S. R. Weiss, and R. S. Baric.** 2002. Systematic assembly of a full-length infectious cDNA of mouse hepatitis virus strain A59. J. Virol. **76:**11065–11078.
49. **Yu, D., and X. Zhang.** 2006. Differential induction of proinflammatory cytokines in primary mouse astrocytes and microglia by coronavirus infection. Adv. Exp. Med. Biol. **581:**407–410.